Translational Oncology
www.transonc.com

Volume 2 Number 1 March 2009 pp. 31–38 31

X Box–Binding Protein 1 Regulates Angiogenesis in Human Pancreatic Adenocarcinomas[1,2]

Lorenzo Romero-Ramirez*, Hongbin Cao*, Maria Paz Regalado*, Neeraja Kambham†, Dietmar Siemann‡, Jeff J. Kim*, Quynh T. Le* and Albert C. Koong*

*Department of Radiation Oncology, Stanford University, Stanford, CA 94305-5152, USA; †Department of Pathology, Stanford University, Stanford, CA 94305-5152, USA; ‡Department of Radiation Oncology, University of Florida, Gainesville, FL, USA

Abstract

PURPOSE: Tumors encounter endoplasmic reticulum stress during tumor growth and activate an adaptive pathway known as the unfolded protein response (UPR). Because this pathway is induced by the tumor microenvironment, it is a promising target for cancer therapy. We have previously demonstrated that X-box binding protein 1 (XBP-1), a key regulator of the UPR, was required for survival under hypoxia and critical for tumor growth in tumor xenografts. In this study, we investigated the role of XBP-1 in regulating tumor angiogenesis. *METHODS:* We used an intradermal angiogenesis model to quantify the effect of XBP-1 on angiogenesis. We also used a human tumor xenograft model to assay for tumor growth delay. We determined vascular endothelial growth factor (VEGF) expression by quantitative polymerase chain reaction and ELISA. Finally, we stained human pancreatic adenocarcinoma specimens for XBP-1 expression and correlated the expression pattern of XBP-1 with CD31 (endothelial cell marker) expression. *RESULTS:* We demonstrated that XBP-1 is essential for angiogenesis during early tumor growth. Inhibiting XBP-1 expression by short-hairpin RNA sequence specific for XBP-1 reduced blood vessel formation in tumors from mouse embryonic fibroblast cells and human fibrosarcoma tumor cells (HT1080). Expressing a dominant-negative form of IRE1α also reduced blood vessel formation in tumors. Moreover, expression of spliced XBP-1 (XBP-1s) restored angiogenesis in IRE1α dominant-negative expressing cells. We further demonstrated that XBP-1–mediated angiogenesis does not depend on VEGF. *CONCLUSIONS:* We propose that the IRE1α–XBP-1 branch of the UPR modulates a complex proangiogenic, VEGF-independent response that depends on signals received from the tumor microenvironment.

Translational Oncology (2009) 2, 31–38

Introduction

Tumors experience hypoxia and endoplasmic reticulum (ER) stress during growth when the energy demands exceed the capacity of the vasculature to supply nutrients. Under these pathophysiological conditions, activation of the unfolded protein response (UPR) triggers an adaptive pathway that allows cells to survive in this microenvironment characterized by hypoxia, low glucose, and low pH. Inhibiting the UPR under these conditions is a promising therapeutic strategy [1,2].

We have previously demonstrated that the IRE1-XBP1 branch of the UPR mediated survival under hypoxia and was essential for tumor growth. Transformed mouse embryonic fibroblasts (MEFs) [3] or human fibrosarcoma tumor cells (HT1080) [4] that are deficient in X-box binding protein 1 (XBP-1) are impaired in their ability to grow as tumor xenografts in SCID mice. Similarly, PKR-like ER kinase (PERK), another branch of the UPR responsible for attenuation of protein translation during hypoxia and ER stress, also plays an important role in regulating tumor growth [5,6]. Both PERK and XBP-1–deficient cells showed increased apoptosis and decreased clonogenic

Address all correspondence to: Albert C. Koong, 269 Campus Dr West, CCSR-1245C, Stanford, CA 94305-5152. E-mail: akoong@stanford.edu
[1]This work was supported by PO1 CA67166 (Q.T.L. and A.C.K.).
[2]This article refers to supplementary materials, which are designated by Figures W1 to W3 and are available online at www.neoplasia.com.
Received 11 November 2008; Revised 31 December 2008; Accepted 6 January 2009

DOI 10.1593/tlo.08211

survival during ER stress/hypoxia. These findings strongly suggest that the UPR represents an important signaling pathway that is critical for tumor growth.

UPR target genes are expressed in a variety of human tumors [7] and have important implications in cancer therapy [8,9]. XBP-1 has been reported to be overexpressed in breast cancer [10], hepatocellular carcinoma [11], and colorectal cancer [12]. In this study, we investigated the role of XBP-1 in regulating tumor angiogenesis.

Materials and Methods

Cell Culture and Hypoxia Treatments

MEF and human HT1080 fibrosarcoma cells were maintained in Dulbecco's modified Eagle's medium supplemented with fetal bovine serum (10%) at 37°C in a 5% CO_2 incubator. For the hypoxia experiments, cells were treated at 70% to 80% confluency and maintained in an anaerobic chamber (Sheldon Corp., Cornelius, OR) with P_{O_2} levels <0.02%.

Constructs, Reporter Assays, and Production of Stably Expressing Cells

Human XBP-1–specific sequence (5′-GCTCTTTCCC TCATGTATACT-3′) was used for short-hairpin RNA (shRNA) and cloned in pSIREN-RetroQ vector (Clontech, Mountain View, CA). We used the following sequences as shRNA controls: scrambled (SC; 5′-CACATGTTCCGATCTCGGC-3′), nontarget sequence obtained from Sigma-Aldrich, St. Louis, MO (NT; 5′-CAACAAGATGAAGAGCACCAA-3′), green fluorescent protein sequence (GFP; 5′-TACAACAGCCACAACGTCTAT-3′), and a sequence with four mismatches of the human XBP-1–specific sequence (MM; 5′-GCTgTaTgCCTgATGTATACT-3′).

Additional details are available in Supplementary Material. A flag-tagged dominant-negative form of IRE1α and the XBP-1 spliced form (XBP-1s) was cloned into pBabe-Puromycin and pWZL-hygromycin retroviral vectors, respectively. Infected cells were selected with hygromycin (375 μg/ml) or puromycin (1 μg/ml) for 10 days. The expression of XBP-1 was confirmed by Western blot analysis, quantitative polymerase chain reaction (qPCR), and the UPRE-Luciferase reporter assay techniques as described below. HT1080 cells (1.5×10^5) were cultured in 12-well plates. The next day, cells were cotransfected with a pGL3-5×UPRE-luc (containing five repetitions of the XBP-1 DNA binding site), and a plasmid containing the β-galactosidase enzyme was used for transfection efficiency. All data were normalized by β-galactosidase activity and expressed as a ratio of luciferase/β-galactosidase activity. All results were normalized to the control whose value was arbitrarily set to 1. Lipofectamine and Plus reagent were used according to the manufacturer's protocol (Invitrogen, Carlsbad, CA). Luciferase assay kit and β-galactosidase assay kit were used according to the manufacturer's protocol (Promega, San Luis Obispo, CA).

Western Blot Analysis

Cell extracts were prepared in 9 M urea–75 mM Tris-HCl (pH 7.5) and 0.15 M β-mercaptoethanol (Sigma, St. Louis, MO), sonicated briefly, boiled at 95°C for 5 minutes, and loaded onto SDS-PAGE gels. After electrophoresis, the proteins were transferred onto a nitrocellulose membrane (Bio-Rad, Hercules, CA) and blocked in 5% nonfat milk with 0.1% Tween-20 in Tris-buffered saline for 30 minutes at room temperature. An affinity-purified rabbit polyclonal antibody, generated against a peptide fragment specific for human XBP-1s, was used at 1:1000 dilution or a rabbit polyclonal antibody from Biolegend (San Diego, CA) at 1:500 dilution. A monoclonal β-actin antibody (1:3000; Sigma) was used for loading control. After incubation with the primary antibody, the membranes were washed and hybridized with peroxidase-conjugated IgG antibodies (Jackson Immunoresearch, West Grove, PA) as secondary antibodies. The blots were developed with enhanced chemoluminiscence (ECL) substrate (Amersham, Piscataway, NJ).

Quantitative PCR

Total RNA was extracted from cultured cells using TRIzol reagent. The cDNA was synthesized from 2 μg of total RNA using Superscript III Reverse Transcriptase kit (Invitrogen) according to the manufacturer's protocol. The cDNA was subjected to qPCR on an ABI PRISM 7900HT (Applied Biosystems, Foster City, CA) using SYBR Green PCR Kit. PCR amplifications were performed with specific primers in a total volume of 10 μl containing 1 μl of sense and antisense primer mixture (5 μM of each primer), 5 μl of 2xSYBR Green QPCR Master Mix (Applied Biosystems), 1 μl of diluted cDNA and nuclease-free PCR-grade water. The mixture was used as a template for the amplification after initial denaturation at 95°C and 40 cycles (95°C for 30 seconds, 60°C for 1 minute, and 72°C for 30 seconds). Primers sequences used were as follows: for human XBP-1, 5′-AGCCAAGGGGAATGAAGTGA-3′ (sense) and 5′-GGGGAAGGGCATTTGAAGAA-3′ (antisense); for mouse XBP-1, 5′-TCCGCAGCACTCAGACTATG -3′ (sense) and 5′-ACAGGGTCCAACTTGTCCAG-3′ and for human VEGF 5′-ATCTTCAAGCCATCCTGTGTGC-3′ (sense) and 5′-GCTCACCGCCTCGGCTTGT-3′ (antisense). SYBR Green fluorescence was measured, and quantification of each PCR product was expressed relative to beta-actin or 18S rRNA.

Angiogenesis Assay In Vivo

Each SCID mouse was implanted intradermally on the ventral surface with four tumors symmetrically equidistant as described by Danielsen and Rofstad [13]. Cells (1×10^5 for MEF cells and 2×10^5 for HT1080 cells) were injected in a volume of 10 μl together with one drop of 0.4% trypan blue to visualize the sites of injection. After 3 and 6 days for MEF cells or after 7 days for HT1080 cells, the mice were killed, the skin carefully separated, and the number of vessels reaching the edge of the tumor was scored by independent observers blinded to the treatment group with the use of a dissecting microscope at 15× magnification. Results from different controls for shRNA are included in Supplementary Material. Uninfected parental HT1080 cells were used as an additional control.

VEGF Secretion Assay

Cells (4×10^5) were seeded in 6-cm dishes and incubated overnight. Fresh media were added, and cells were exposed to 24 hours of normoxia or hypoxia (O_2 < 0.02%). VEGF was measured by ELISA according to the manufacturer's protocol (R&D Systems, Indianapolis, IN).

Immunohistochemical Staining

The immunohistochemical stains were performed using an affinity-purified rabbit polyclonal antibody, generated against a peptide fragment specific for human XBP-1s antibody directed against human XBP-1. Serial sections of 4 μm were obtained from the selected paraffin blocks, deparaffinized in xylene, and hydrated in a graded series

of alcohol. Heat-induced antigen retrieval was carried out by microwave pretreatment in citric acid buffer (10 mM, pH 6.0) for 10 minutes. The XBP-1s antibody was used at a dilution of 1:1000, and the tissue was incubated at room temperature for 30 minutes. The endogenous peroxidase was blocked, and the DAKO Envision system (DAKO Corporation, Carpinteria, CA) was used for detection. A tissue microarray of formalin-fixed paraffin-embedded normal and carcinoma tissues was used for initial titration of the XBP-1 antibody. On the basis of these results, colon carcinoma was selected as a positive control, and normal colon mucosa was used as a negative control. The XBP-1 staining was scored semiquantitatively in the invasive carcinoma, stroma within the carcinoma, and nonneoplastic pancreas as follows: 0, no staining; 1+, weak and focal (<10% of lesional cells positive); 2+, patchy weak or strong staining (10-30% of lesional cells positive); 3+, strong and diffuse (>30% of lesional cells positive).

Results

XBP-1 Is Essential for Tumor Angiogenesis in MEF Cells and in Human Fibrosarcoma HT1080 Cells

We have previously demonstrated that constitutive XBP-1 deficiency impairs tumor growth in human and mouse cell lines [3,4]. In this study, we used an intradermal angiogenesis assay [13] to determine the role of XBP-1 on tumor angiogenesis. We expressed a shRNA sequence to inhibit XBP-1 expression (Figure 1*A*) in mouse embryonic fibroblasts (shXBP-1 MEF) and found that their growth as tumor xenografts were impaired compared with the control cells (Figure 1*B*). The impaired growth of the tumor xenografts expressing shXBP-1 is consistent with the decreased expression of XBP-1 observed in these cells. After implanting these cells intradermally, shXBP-1MEF cells showed significantly less blood vessel formation than the control cells (shControl MEF; Figure 1*C*). In these studies, we implanted 1×10^5 cells and had two independent observers score the number of tumor capillaries for each tumor using a dissection microscope. Each observer was blinded to the cell type for each tumor. We also performed the same experiments in a human fibrosarcoma cell line (HT1080). As shown in Figure 2*A* (*right panel*), the shXBP-1HT1080 cells had significantly less XBP-1 protein expression under hypoxic conditions than the control cells. Similarly, using an XBP-1 responsive reporter construct (5×-UPRE-luciferase), cells inhibited in XBP-1 expression also showed less XBP-1–dependent reporter transactivation after treatment with tunicamycin, an inhibitor of glycosylation (Figure 2*A*, *left panel*). Overall, the number of capillaries was significantly reduced in shXBP-1HT1080 cells compared with the control shSC-HT1080 cells (Figure 2, *B* and *C*, and Figure W2). There was no difference in cell proliferation between these cell lines when assayed for growth in cell culture (data not shown). As additional controls to rule out the possibility of "off-target" effects of XBP-1 shRNA, we compared the blood vessel formation of shXBP-1HT1080 cells with several HT1080 control cells expressing a scrambled shRNA sequence, a 4-bp

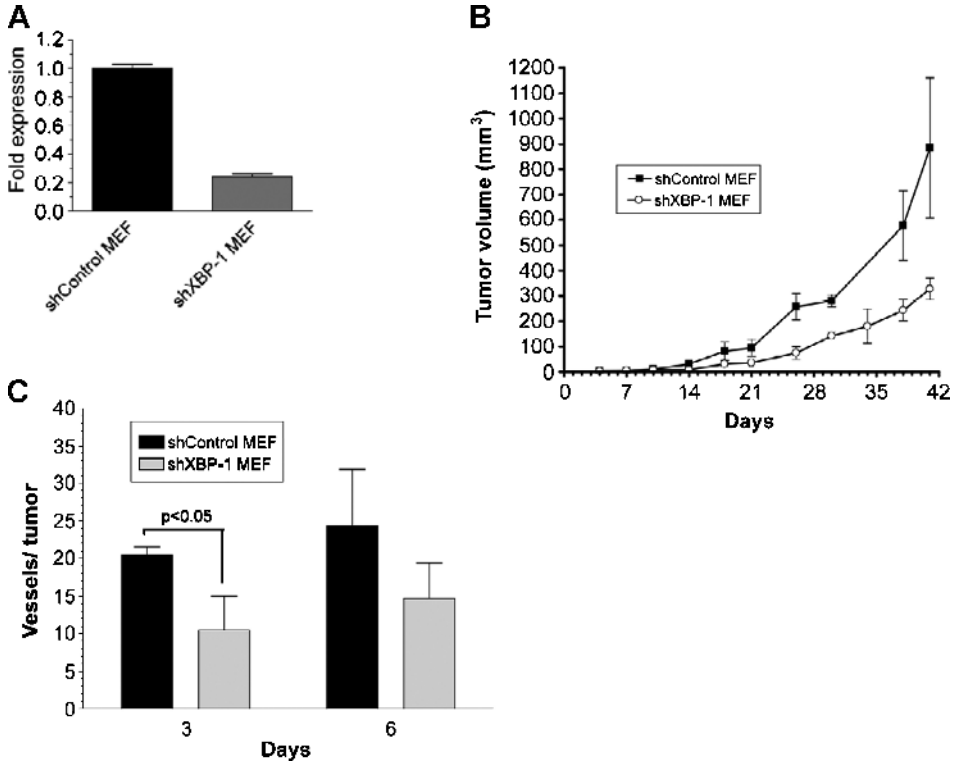

Figure 1. XBP-1 is essential for tumor angiogenesis in MEF cells. (A) Reduction of XBP-1 expression by a short-hairpin specific sequence was verified by qPCR for total XBP-1 messenger. (B) Tumor growth data from XBP-1 control MEF cells (shControl MEF) and XBP-1 shRNA–expressing cells (shXBP-1 MEF). Each SCID mouse was implanted subcutaneously with two tumors consisting of 2×10^6 shControl MEF cells in one flank and 2×10^6 shXBP-1 MEF cells in the contralateral flank. Error bars, SD of the mean from four tumors. (C) Angiogenesis assay *in vivo* for XBP-1 control MEF cells (shControl MEF) and XBP-1 shRNA–expressing cells (shXBP-1 MEF). SCID mice were intradermally implanted with 1×10^5 MEF cells. The number of vessels growing into the tumor was scored 3 and 6 days after implantation with each observer blinded to the treatment condition. Error bars, SE of the mean from at least six tumors. Statistical significance was determined using a 2-tailed *t* test.

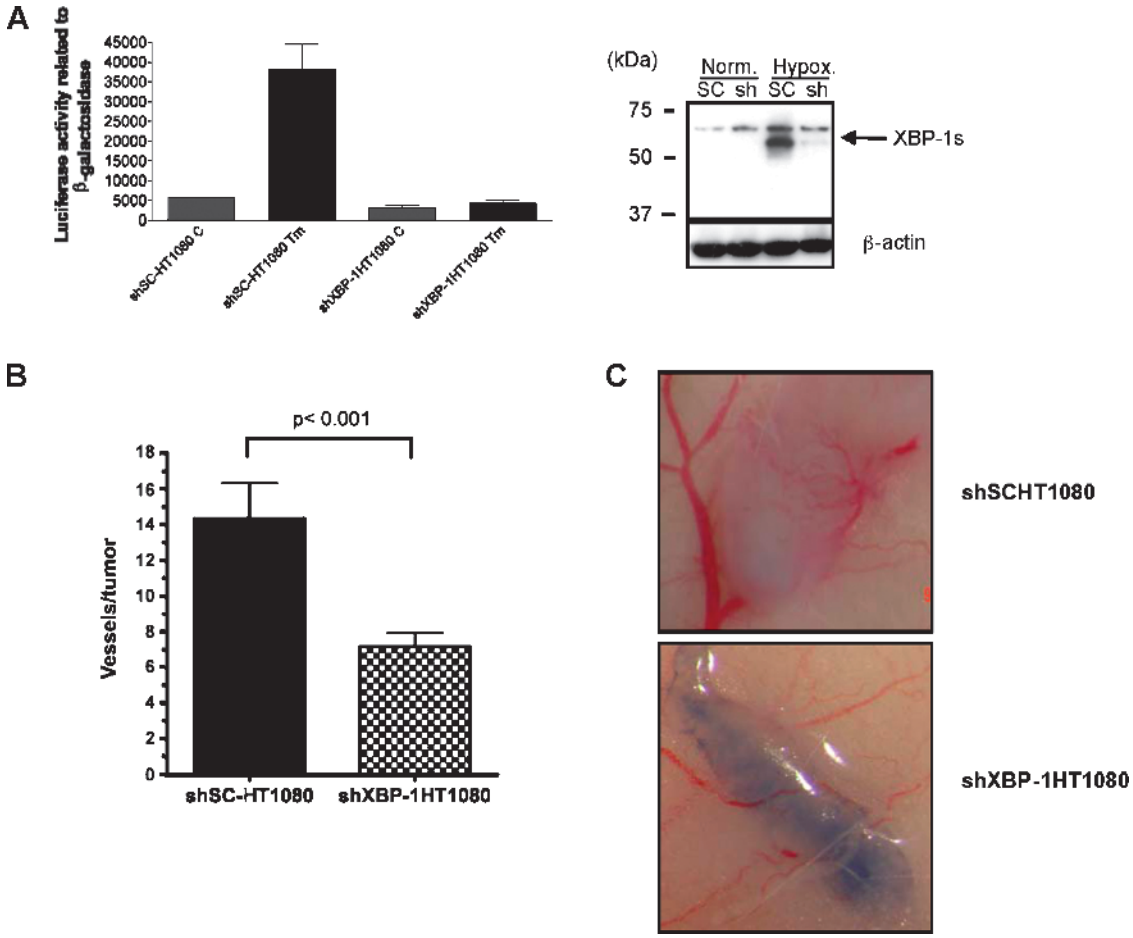

Figure 2. XBP-1 is essential for tumor angiogenesis in HT1080 cells. Reduction of XBP-1 expression by a short-hairpin specific sequence was verified by (A) UPRE reporter assay (left panel) and Western blot analysis for spliced XBP-1 (XBP-1s–specific antibody, right panel). Cells were exposed to 8 hours of tunicamycin (5 μg/ml for 8 hours) for the reporter assays and 24 hours of hypoxia ($O_2 < 0.02\%$) for the Western blot analysis to induce XBP-1 splicing. Expression of β-actin is included as a loading control. (B) Angiogenesis assay *in vivo* for XBP-1 scramble control HT1080 cells (shSc-HT1080) and XBP-1 shRNA–expressing cells (shXBP-1HT1080). SCID mice were intradermally implanted with 2×10^5 HT1080 cells. The number of vessels growing into the tumor was scored 7 days after implantation. Each observer quantitated the number of blood vessels independently and was blinded to the treatment condition. Error bars, SE of the mean from at least 10 tumors. Statistical significance was determined using a 2-tailed *t* test. (C) Representative photomicrographs of the tumors from angiogenesis assays. As shown in the bottom panel, there are significantly fewer capillaries growing into the HT1080 tumors with reduced XBP-1 expression (sh-XBP-1HT1080) compared with the scrambled shRNA control–expressing cells (top panel, shSCHT1080).

mismatch of the original knockdown sequence, a non target shRNA sequence, a GFP shRNA sequence, and uninfected HT1080 parental cells (Figure 2*B* and Figure W2). Functionally, only the shXBP-1HT1080 cells were able to block transactivation of an XBP-1–dependent reporter construct (UPRE-luciferase; Figure W1). We have previously demonstrated that HT1080 cells expressing XBP-1 shRNA are inhibited in tumor growth compared with control HT1080 cells [14]. Collectively, these studies demonstrate that specific inhibition of XBP-1 results in decreased tumor growth and decreased angiogenesis.

IRE1α Is Essential for Tumor Angiogenesis in HT1080 Cells

XBP-1 protein has two isoforms that are expressed from the same mRNA: an unspliced (XBP-1u) and spliced form (XBP-1s). Under hypoxia and ER stress conditions, XBP-1 mRNA is spliced by the ER protein IRE1α. To determine the role of IRE1α on angiogenesis, we overexpressed a truncated version of this protein that contained only the carboxy terminus. Expression of this dominant-negative form of IRE1α inhibited the induction of XBP-1 splicing under hypoxia (Figure 3*A*). Using the same intradermal angiogenesis assays, cells expressing this dominant-negative form of IRE1α (HT1080-IΔC), also demonstrated fewer capillaries than control cells (HT1080-pBabe; Figure 3*B*). Because IRE1α is required for XBP-1 splicing, these results suggest a key role for both IRE1α and spliced XBP-1 in tumor angiogenesis.

XBP-1s Restores Tumor Angiogenesis in IRE1α Dominant-Negative Expressing Cells

We generated additional HT1080 cell lines expressing dominant-negative IRE1α alone (ΔC), spliced XBP-1 alone (S), or both simultaneously (ΔCS). Spliced XBP-1 expression was confirmed by Western blot analysis with an antibody that only recognizes the spliced form (Figure 4*A*, *top panel, lanes 3, 4, 7, and 8*). Dominant-negative IRE1α expression (Flag-tagged) was confirmed with anti-Flag antibody (Figure 4*A*, *lower panel, lanes 2, 3, 6, 7*). As expected in control cells, tunicamycin induced XBP-1 splicing (compare *top panel, lane 1 vs 5*),

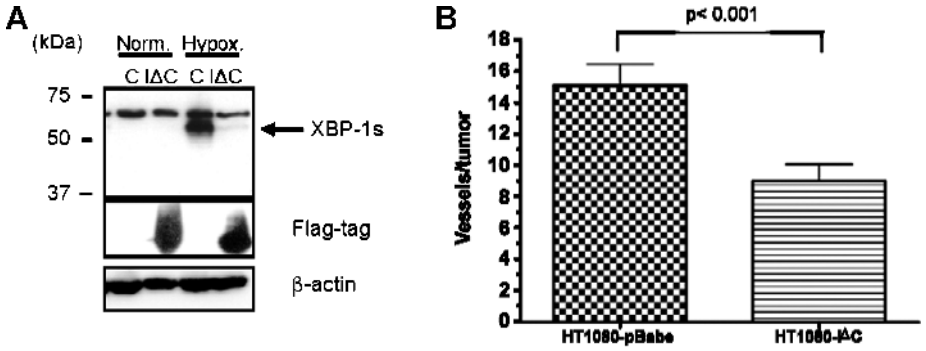

Figure 3. A dominant-negative form of IRE1α inhibits angiogenesis in HT1080 cells. (A) Western blot for spliced XBP-1 (XBP-1s), Flag-tagged IRE1α dominant-negative protein (IΔC), and β-actin (as loading control). Cells were treated with 24 hours of hypoxia ($O_2 < 0.02\%$) to induce XBP-1 splicing. There was no XBP-1 splicing in the IRE1α dominant-negative expressing cells. (B) Angiogenesis assay *in vivo* for empty vector control cells (HT1080-pBabe) and flag-tagged IRE1α dominant-negative expressing cells (HT1080-IΔC). Error bars, SE of the mean from 10 tumors. Statistical significance was determined using a 2-tailed *t* test.

and XBP-1 splicing was blocked when dominant-negative IRE1α was expressed (compare *top panel, lane 2 vs 6*). Figure 4*B* shows that an XBP-1–responsive reporter construct (5×-UPRE-luciferase) was blocked by dominant-negative IRE1α expression (*middle columns*) and that this inhibition can be overcome with overexpression of spliced XBP-1 (*far right columns*). And finally, HT1080 cells expressing dominant-negative IRE1α (HT1080dvector-ΔC) demonstrated reduced blood vessel formation compared with the control cells (HT1080dvector-φ). However, cells coexpressing dominant-negative IRE1α and spliced XBP-1 (HT1080dvector-ΔCS) restored angiogenesis to similar levels as the control cells (HT1080dvector-φ; Figure 4*C*). Next, we determined whether XBP-1 expression influenced VEGF expression in these cells. Using qPCR, we did not observe any difference in either basal VEGF expression or hypoxic induction of VEGF expression between HT1080 control cells (shSC-HT1080) and HT1080 cells expressing an XBP-1 shRNA construct (shXBP-1HT1080; Figure 4*D*). Similar findings were noted for SU86.86 cells, a human pancreatic cancer cell line. VEGF protein secretion was also not significantly different between these cell lines under normoxic and hypoxic conditions (Figure W3). These studies suggest that although XBP-1s plays an important role in angiogenesis, the regulation of this process occurs independently of VEGF.

XBP-1 Expression in Human Pancreatic Tumors Correlates with CD31 Expression

Because of the inherent limitations of the animal models of angiogenesis used, we further extended our studies of XBP-1s–mediated angiogenesis in a defined set of human pancreatic tumors. We stained 32 consecutive human pancreatic adenocarcinoma resection specimens (mucinous tumors excluded) for spliced XBP-1 and CD31 (endothelial cell marker) expression. In general, the XBP-1s staining was specific for the tumor cells, whereas the CD31 staining tended to localize to the tumor stromal cells. Neither did we find a correlation between pancreatic tumor size and XBP-1s expression nor did we observe a correlation between CD31 staining and pancreatic tumor size. Table 1 shows the pathologic characteristics of the pancreatic tumor samples used in this study. A board-certified pathologist (N.K.) scored the intensity of XBP-1s staining in these sections as follows: 0 (no expression), 1 (weak expression), 2 (moderate expression), and 3 (strong expression). On consecutive sections, these specimens were also assessed for CD31 staining. Shown in Figure 5*A* are representative staining of two adjacent pancreatic tumor sections showing high XBP-1s expression from the tumor cells with high CD31 staining from the adjacent stroma. CD31-positive blood vessels were counted at 300× magnification from three different areas within each tumor, and a mean CD31 score was determined for each tumor. We found a significant correlation between XBP-1 staining and mean CD31 score within these tumors. Specifically, the group of patients with mod-strong XBP-1s expression had higher CD31 scores than those patients with neg-weak XBP-1s expression (Figure 5*B*). These results indicate that XBP-1 expression in human pancreatic tumors is clinically relevant to angiogenesis and suggests a therapeutic opportunity in treating this disease.

Discussion

We have previously reported that human pancreatic tumors are extremely hypoxic as determined by intraoperative measurements using a polar graphic microelectrode technique [15]. What remains unclear is whether tumor angiogenesis occurs as a response to tumor hypoxia or whether tumor hypoxia is a consequence of insufficient angiogenesis. Most likely, within human tumors, both processes occur and a dynamic interplay exists between the tumor microenvironment and angiogenesis. The ultimate consequence of this interaction is tumor growth.

In prior studies, we found that XBP-1 was a critical mediator of tumor growth, and the data from the current study support the hypothesis that at least part of the mechanism for impaired growth of XBP-1 deficient tumors was through decreased angiogenesis. Our previous study demonstrated that VEGF secretion was not significantly different between XBP-1 wild-type and knockout MEFs [3], suggesting that VEGF does not play a direct role in XBP-1–regulated angiogenesis. In the current study, we also did not observe any significant differences in VEGF expression in two different tumor cell lines (HT1080, human fibrosarcoma, and SU.86.86, human pancreatic cancer) expressing shRNA constructs to block XBP-1 (Figure 4*D* and Figure W3). However, angiogenesis is a complex sequence of events, and up-regulation of other proangiogeneic factors as well as down-regulation of antiangiogeneic factors also plays an important role. With regards to other UPR signaling pathways, PERK has also been implicated in tumor growth and angiogenesis [16]. Interestingly, VEGF secretion also was not regulated in a PERK-dependent manner [5].

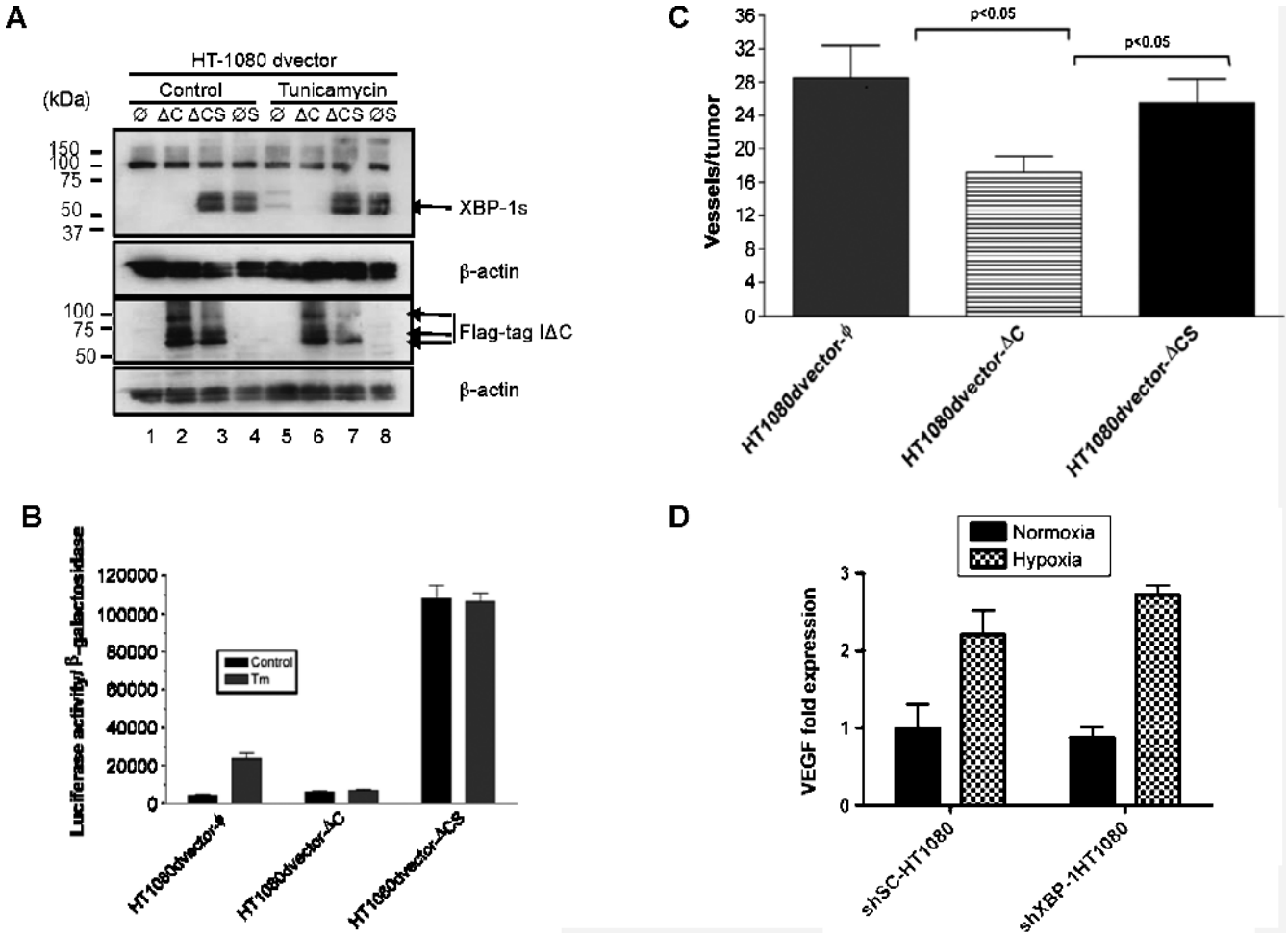

Figure 4. XBP-1 spliced form (XBP-1s) rescues tumor angiogenesis in IRE1α dominant-negative expressing cells. (A) Expression of XBP-1s and IRE1α dominant-negative in HT1080 cells was confirmed by Western blot analysis. Lanes 1 and 5 are HT1080 vector control cells. Lanes 2 and 6 are HT1080 cells transfected with a Flag-tagged IRE1α dominant-negative construct. Lanes 3 and 7 are HT1080 cells transfected with both Flag-tagged IRE1α dominant-negative construct and an XBP-1 overexpression construct. Lanes 4 and 8 are HT1080 cells transfected with XBP-1 overexpression construct. Tunicamycin (5 μg/ml for 8 hours) was used to induce XBP-1 splicing. β-Actin was used as a loading control. Western blot analysis was carried out using XBP-1s–specific antibody (Biolegend). (B) XBP-1 reporter (UPRE-luciferase) assay in HT1080 cells expressing vector alone (vector-φ), IRE1α dominant-negative (vector-ΔC), or IRE1α dominant-negative and spliced XBP-1 (ΔCS). All cells were treated with tunicamycin (5 μg/ml for 8 hours). Expression of IRE1α dominant-negative blocked transactivation of the UPRE-luciferase reporter during tunicamycin treatment. Inhibition of the UPRE-luciferase reporter could be reversed by overexpression of XBP-1s. (C) Angiogenesis assay for HT1080 cells expressing vector alone (vector-φ), IRE1α dominant-negative (φ-ΔC), or IRE1α dominant-negative and spliced XBP-1 (ΔCS). Error bars, SE of the mean from at least eight tumors. Statistical significance was determined using a 2-tailed *t* test. (D) VEGF expression by qPCR in HT1080 control cells (shSC-HT1080) or HT1080 cells inhibited in XBP-1 expression by shRNA (shXBP-1HT1080). There was no difference in VEGF expression at baseline or during hypoxia between these two cell lines.

Table 1. Pancreatic Adenocarcinoma Tumor Characteristics (n = 32).

Patients' age (years), mean (range)	69 (43-85)
Tumor grade, *n* (%)	
Well differentiated	7 (22)
Moderately differentiated	19 (59)
Poorly differentiated	6 (19)
Lymph node status, *n* (%)	
Positive	16 (50)
Negative	16 (50)
Resection margin, *n* (%)	
Positive	10 (31)
Negative	22 (69)
Tumor size (cm), median (range)	3.80 (1.10-6.00)

The cytoplasmic portion of IRE1α contains both a kinase and an endonuclease domain. Whereas the kinase domain is required for the endonuclease activity of the protein, it can also activate the JNK pathway through its interaction with TRAF2 [17]. The IRE1 endonuclease is responsible for splicing XBP-1 and has also been shown to degrade a set of target mRNA in *Drosophila*, including some mRNA that encode for proteins involved in angiogenesis [18]. Drogat et al. showed that in cell culture, tumor cells expressing a kinase inactive mutant for IRE1α (IRE1αK599A) had decreased VEGF mRNA induction during relatively mild hypoxia (3% O_2) or hypoglycemia [19]. Furthermore, these investigators used an orthotopic glioma tumor model

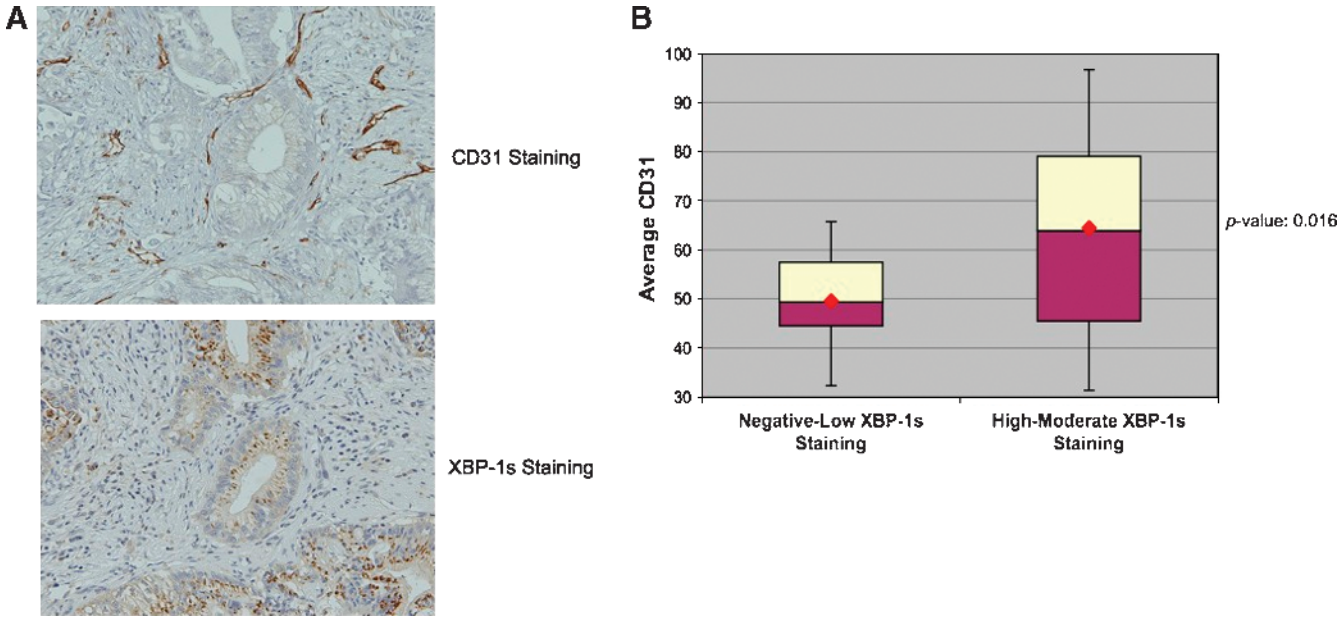

Figure 5. VEGF mRNA expression is not regulated by XBP-1. (A) The top panel shows strong CD31 staining of endothelial cells in a human pancreatic adenocarcinoma. The bottom panel is an adjacent pancreatic tumor section showing strong XBP-1s expression. (B) Thirty-two consecutive pancreatic tumor resection specimens were stained for CD31 and XBP-1s expression. We found a strong correlation between XBP-1s staining and CD31 staining ($P = .016$) suggesting that XBP-1s is a clinically relevant to angiogenesis in pancreatic cancer.

to show that IRE1αK599A expressing tumors grew slower and showed decreased blood vessel formation compared with control tumors.

Our data are consistent with these investigators and also demonstrate that IRE1α plays an important role in angiogenesis. In both tumor model systems, overexpression of a dominant-negative form of IRE1α resulted in reduced blood vessel formation. Moreover, overexpression of spliced XBP-1 was sufficient to overcome the effect of IRE1α dominant-negative expression on angiogenesis. However, our findings differ from Drogat et al. in that we did not observe any significant differences in VEGF expression in two different cell lines inhibited in XBP-1 expression (Figure 4*D* and Figure W3). These results suggest that VEGF expression may be altered depending on whether XBP-1 or IRE1α is blocked. Another possibility is that these differences may be accounted for by the different cell types used in these experiments. Because the XBP-1 shRNA experiments blocked expression of both the spliced and unspliced form of XBP-1, we cannot exclude the possibility that the unspliced form of XBP-1 may also contribute to angiogenesis. Although unspliced XBP-1 can function as a negative regulator of spliced XBP-1 [20,21], it may also differentially activate UPR target genes if its stability is altered [22].

Our results demonstrate that XBP-1 expression is important for angiogenesis in a variety of tumor xenografts derived from multiple different cell types including MEFs and HT1080 cells. These data suggest that our results may be generally applied to multiple tumor types. Moreover, we report a strong correlation between XBP-1 activation and increased vessel density from human pancreatic adenocarcinoma specimens, which strongly suggests that this pathway is relevant in human cancer. And finally, although multiple factors can affect tumor growth (proliferation, apoptosis, adaptation), angiogenesis is an important component of the tumor microenvironment that influence overall tumor growth kinetics. We propose that IRE1/XBP-1 functions as part of a complex network of UPR signaling that depends on the tumor microenvironment for the appropriate angiogenic stimuli. These data have important implications in developing antiangiogenic tumor treatment strategies in pancreatic cancers.

Acknowledgments

The authors thank the members of Koong and Le Laboratory for their comments and suggestions.

References

[1] Feldman DE, Chauhan V, and Koong AC (2005). The unfolded protein response: a novel component of the hypoxic stress response in tumors. *Mol Cancer Res* **3**, 597–605.

[2] Ma Y and Hendershot LM (2004). The role of the unfolded protein response in tumour development: friend or foe? *Nat Rev Cancer* **4**, 966–977.

[3] Romero-Ramirez L, Cao H, Nelson D, Hammond E, Lee AH, Yoshida H, Mori K, Glimcher LH, Denko NC, Giaccia AJ, et al. (2004). XBP1 is essential for survival under hypoxic conditions and is required for tumor growth. *Cancer Res* **64**, 5943–5947.

[4] Chen Y, Feldman DE, Deng C, Brown JA, De Giacomo AF, Gaw AF, Shi G, Le QT, Brown JM, and Koong AC (2005). Identification of mitogen-activated protein kinase signaling pathways that confer resistance to endoplasmic reticulum stress in *Saccharomyces cerevisiae*. *Mol Cancer Res* **3**, 669–677.

[5] Bi M, Naczki C, Koritzinsky M, Fels D, Blais J, Hu N, Harding H, Novoa I, Varia M, Raleigh J, et al. (2005). ER stress–regulated translation increases tolerance to extreme hypoxia and promotes tumor growth. *EMBO J* **24**, 3470–3481.

[6] Koumenis C, Naczki C, Koritzinsky M, Rastani S, Diehl A, Sonenberg N, Koromilas A, and Wouters BG (2002). Regulation of protein synthesis by hypoxia via activation of the endoplasmic reticulum kinase PERK and phosphorylation of the translation initiation factor eIF2alpha. *Mol Cell Biol* **22**, 7405–7416.

[7] Li J and Lee AS (2006). Stress induction of GRP78/BiP and its role in cancer. *Curr Mol Med* **6**, 45–54.

[8] Fels DR and Koumenis C (2006). The PERK/eIF2alpha/ATF4 module of the UPR in hypoxia resistance and tumor growth. *Cancer Biol Ther* **5**, 723–728.

[9] Koong AC, Chauhan V, and Romero-Ramirez L (2006). Targeting XBP-1 as a novel anti-cancer strategy. *Cancer Biol Ther* **5**, 756–759.

[10] Fujimoto T, Onda M, Nagai H, Nagahata T, Ogawa K, and Emi M (2003). Upregulation and overexpression of human X-box binding protein 1 (hXBP-1) gene in primary breast cancers. *Breast Cancer* **10**, 301–306.

[11] Shuda M, Kondoh N, Imazeki N, Tanaka K, Okada T, Mori K, Hada A, Arai M, Wakatsuki T, Matsubara O, et al. (2003). Activation of the *ATF6*, *XBP1* and

grp78 genes in human hepatocellular carcinoma: a possible involvement of the ER stress pathway in hepatocarcinogenesis. *J Hepatol* **38**, 605–614.

[12] Fujimoto T, Yoshimatsu K, Watanabe K, Yokomizo H, Otani T, Matsumoto A, Osawa G, Onda M, and Ogawa K (2007). Overexpression of human X-box binding protein 1 (XBP-1) in colorectal adenomas and adenocarcinomas. *Anticancer Res* **27**, 127–131.

[13] Danielsen T and Rofstad EK (1998). VEGF, bFGF and EGF in the angiogenesis of human melanoma xenografts. *Int J Cancer* **76**, 836–841.

[14] Chen Y, Shi G, Xia W, Kong C, Zhao S, Gaw AF, Chen EY, Yang GP, Giaccia AJ, Le QT, et al. (2004). Identification of hypoxia-regulated proteins in head and neck cancer by proteomic and tissue array profiling. *Cancer Res* **64**, 7302–7310.

[15] Koong AC, Mehta VK, Le QT, Fisher GA, Terris DJ, Brown JM, Bastidas AJ, and Vierra M (2000). Pancreatic tumors show high levels of hypoxia. *Int J Radiat Oncol Biol Phys* **48**, 919–922.

[16] Blais JD, Addison CL, Edge R, Falls T, Zhao H, Wary K, Koumenis C, Harding HP, Ron D, Holcik M, et al. (2006). Perk-dependent translational regulation promotes tumor cell adaptation and angiogenesis in response to hypoxic stress. *Mol Cell Biol* **26**, 9517–9532.

[17] Urano F, Wang X, Bertolotti A, Zhang Y, Chung P, Harding HP, and Ron D (2000). Coupling of stress in the ER to activation of JNK protein kinases by transmembrane protein kinase IRE1. *Science* **287**, 664–666.

[18] Hollien J and Weissman JS (2006). Decay of endoplasmic reticulum–localized mRNAs during the unfolded protein response. *Science* **313**, 104–107.

[19] Drogat B, Auguste P, Nguyen DT, Bouchecareilh M, Pineau R, Nalbantoglu J, Kaufman RJ, Chevet E, Bikfalvi A, and Moenner M (2007). IRE1 signaling is essential for ischemia-induced vascular endothelial growth factor-A expression and contributes to angiogenesis and tumor growth *in vivo*. *Cancer Res* **67** (14), 6700–6707.

[20] Lee AH, Iwakoshi NN, Anderson KC, and Glimcher LH (2003). Proteasome inhibitors disrupt the unfolded protein response in myeloma cells. *Proc Natl Acad Sci USA* **100**, 9946–9951.

[21] Yoshida H, Oku M, Suzuki M, and Mori K (2006). pXBP1(U) encoded in XBP1 pre-mRNA negatively regulates unfolded protein response activator pXBP1(S) in mammalian ER stress response. *J Cell Biol* **172**, 565–575.

[22] Tirosh B, Iwakoshi NN, Glimcher LH, and Ploegh HL (2006). Rapid turnover of unspliced Xbp-1 as a factor that modulates the unfolded protein response. *J Biol Chem* **281**, 5852–5860.

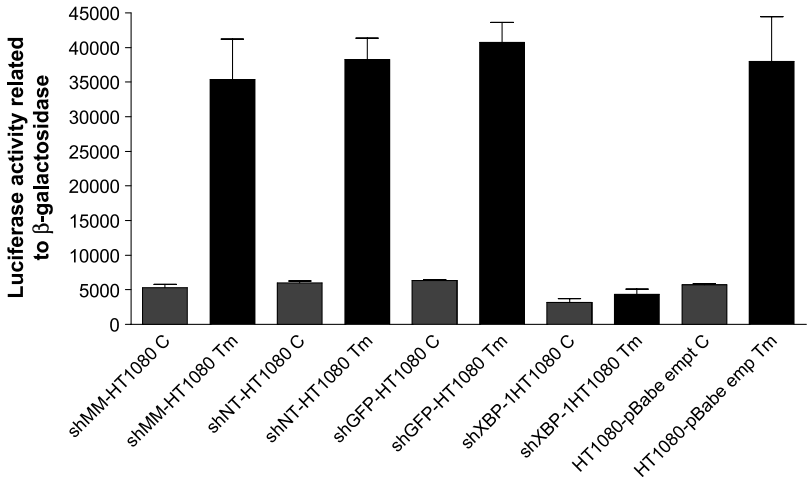

Figure W1. UPRE reporter assays with HT1080 cells expressing different shRNA controls and a specific sequence for XBP-1. UPRE-Luciferase construct and a plasmid containing β-galactosidase (as a transfection control) were transiently transfected in HT1080 cells. UPRE reporter was induced with 4 μg/ml of tunicamycin (Tm) for 8 hours. We used HT1080 cells stably expressing a shRNA sequence specific for XBP-1 (shXBP-1HT1080) and four control sequences as follows: a sequence with four mismatches from the original shRNA-specific sequence for XBP-1 (shMM-HT1080); a nontarget sequence (shNT-HT1080); a sequence from GFP (shGFP-HT1080); and pBabe empty vector–expressing cells (HT1080-pBabe). Error bars, SE of the mean from a triplicate.

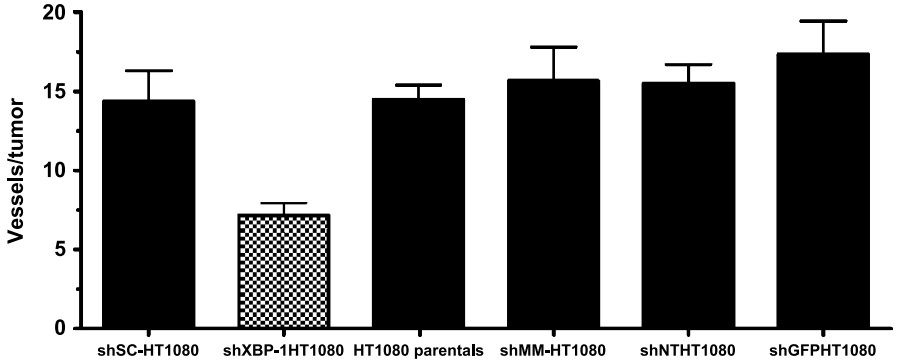

Figure W2. Angiogenesis assays in HT1080 cells stably expressing different shRNA controls and a specific sequence for XBP-1. We used HT1080 cells stably expressing a shRNA specific for XBP-1 (shXBP-1HT1080) and compared blood vessel formation in control cells expressing four different shRNA sequences: a scramble sequence (shSC-HT1080); a sequence with four mismatches from the original shRNA specific for XBP-1 (shMM-HT1080); a nontarget sequence (shNT-HT1080); and a sequence from GFP (shGFP-HT1080). Uninfected HT1080 parental cells were used as additional controls. Error bars, SE of the mean from 10 tumors.

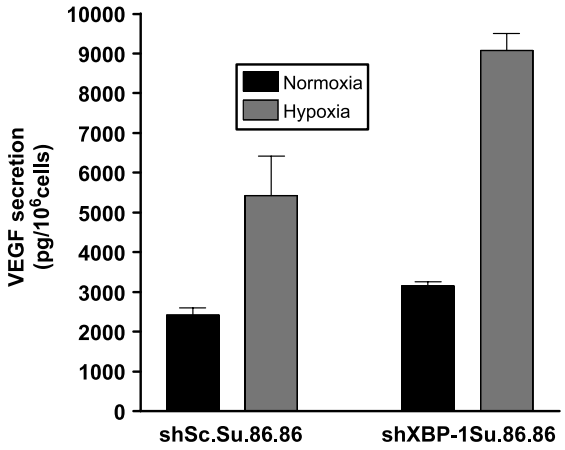

Figure W3. VEGF secretion assay in media conditioned during 24 hours of normoxia or hypoxia ($O_2 < 0.02\%$). There was no difference in VEGF secretion between Su.86.86 shRNA scramble control cells (shSc.Su.86.86) and cells expressing a specific short-hairpin sequence for XBP-1 (shXBP-1Su.86.86). Error bars, SD.